

Effects of synthesis temperature on structural defects of integrated spinel-layered $\text{Li}_{1.2}\text{Mn}_{0.75}\text{Ni}_{0.25}\text{O}_{2+\delta}$: A strategy to develop high capacity cathode material for Li-ion batteries

Ngoc Hung Vu^a, Paulraj Arunkumar^a, Jong Chan Im^a, Duc Tung Ngo^a, Hang T. T. Le^{a,b}, Chan-Jin Park^a, and Won Bin Im^{a,*}

^aSchool of Materials Science and Engineering and Optoelectronics Convergence Research Center, Chonnam National University, 77 Yongbong-ro, Buk-gu, Gwangju 61186, Republic of Korea

^bSchool of Chemical Engineering, Hanoi University of Science and Technology, 1st Dai Co Viet, Hai Ba Trung, Hanoi, Vietnam

*To whom correspondence should be addressed

Tel : +82-62-530-1715

Fax : +82-62-530-1699

E-mail: imwonbin@jnu.ac.kr

Table S1. Refined site occupancy for Li₂MnO₃-like (space group: *C2/m*).

atom	site	occupancy		
		S650	S750	S850
Li (1)	2 <i>b</i>	0.6	0.7	0.78
Mn (1)	2 <i>b</i>	0.2	0.12	0.13
Ni (1)	2 <i>b</i>	0.2	0.18	0.09
Li (2)	2 <i>c</i>	1	1	1
Li (3)	4 <i>h</i>	1	1	1
Mn (2)	4 <i>g</i>	0.85	0.89	0.895
Ni (2)	4 <i>g</i>	0.11	0.06	0.045
Li (4)	4 <i>g</i>	0.15	0.1	0.06
O (1)	4 <i>i</i>	1	1	1
O (2)	8 <i>j</i>	1	1	1

Table S2. Surface area of S650, S750, and S850 obtained by BET method.

sample	surface area (m ² g ⁻¹)
S650	18.866
S750	1.4623
S850	0.6905

The Li⁺ diffusion coefficients of all samples were calculated using the following equation¹ and given in Table S3.

$$D = R^2 T^2 / 2 A n^4 F^4 C^2 \sigma^2 \quad (1)$$

where R is the gas constant, T is the absolute temperature, A is the surface area of the cathode, n is the number of electrons transferred in the half-reaction for the redox couple, F is the Faraday constant, C is the concentration of Li ion in solid, D is the diffusion coefficient (cm² s⁻¹), and σ is the Warburg factor, which is relative to Z' . σ can be obtained from the slope of the lines in Figure S6.

$$Z' = R_D + R_L + \sigma \omega^{-1/2} \quad (2)$$

Table S3. Warburg factor and diffusion coefficient of three samples.

sample	σ	D_{Li^+} (cm ² s ⁻¹)
S650	10.989	5.11×10^{-11}
S750	6.466	1.48×10^{-10}
S850	5.303	2.19×10^{-10}

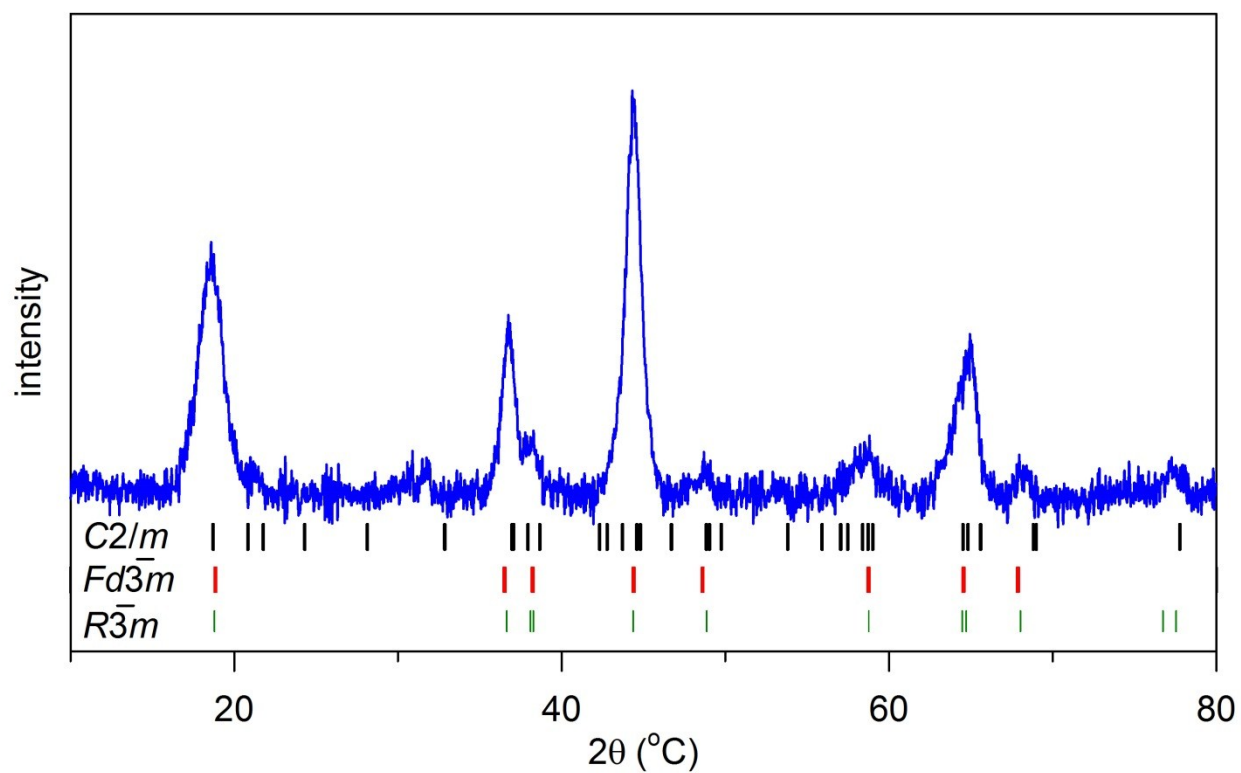


Figure S1. XRD pattern of intermediate product after hydrothermal reaction. The standards marked with $C2/m$ (ICDD entry number 01-084-1634), $Fd\bar{3}m$ (ICDD entry number 01-080-2162), and $R\bar{3}m$ (PDF#09-0063) show the peaks corresponding to Li_2MnO_3 , $\text{LiMn}_{1.5}\text{Ni}_{0.5}\text{O}_4$, and $\text{LiNi}_{0.5}\text{Mn}_{0.5}\text{O}_2$, respectively.

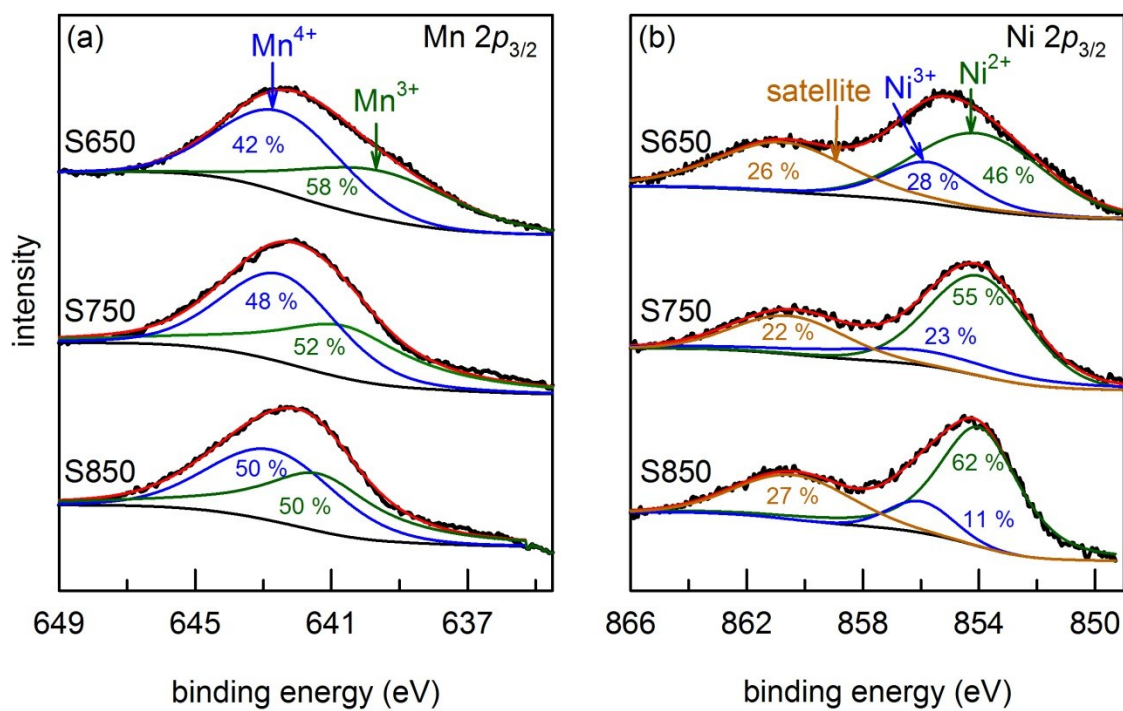


Figure S2. XPS spectra of (a) Mn 2p_{3/2} and (b) Ni 2p_{3/2} with signal deconvolution and assignment to the indicated ions of S650, S750, and S850.

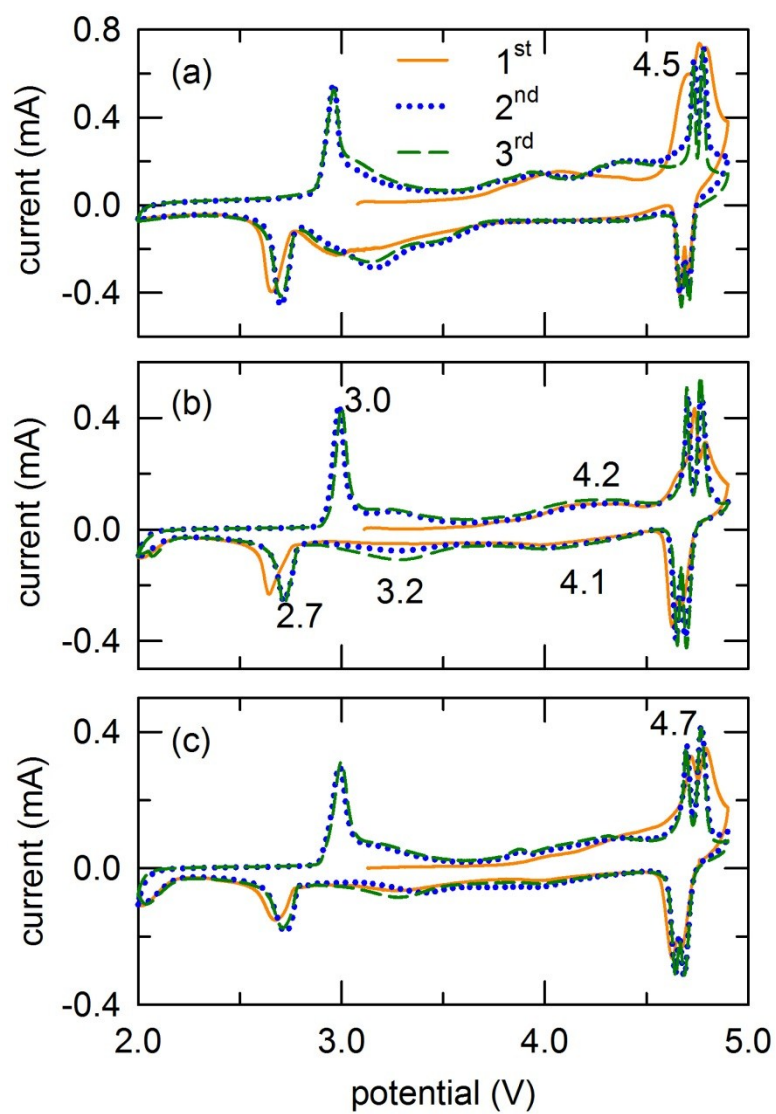


Figure S3. Cyclic voltammograms of (a) S650, (b) S750, and (c) S850 in the potential window of 2.0–4.9 V at a scan rate of 0.05 mVs⁻¹.

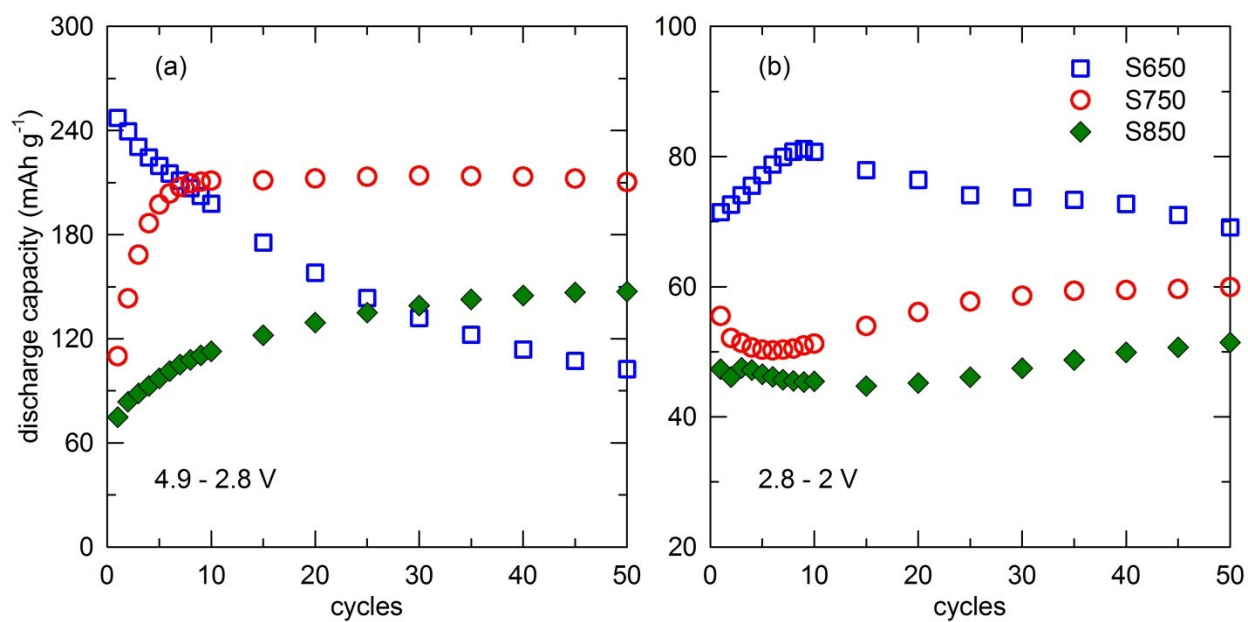


Figure S4. Net discharge capacities in the voltage range of (a) 4.9 – 2.8 V and (b) 2.8 – 2 V of S650, S750, and S850 samples in the first 50 cycles at C/20.

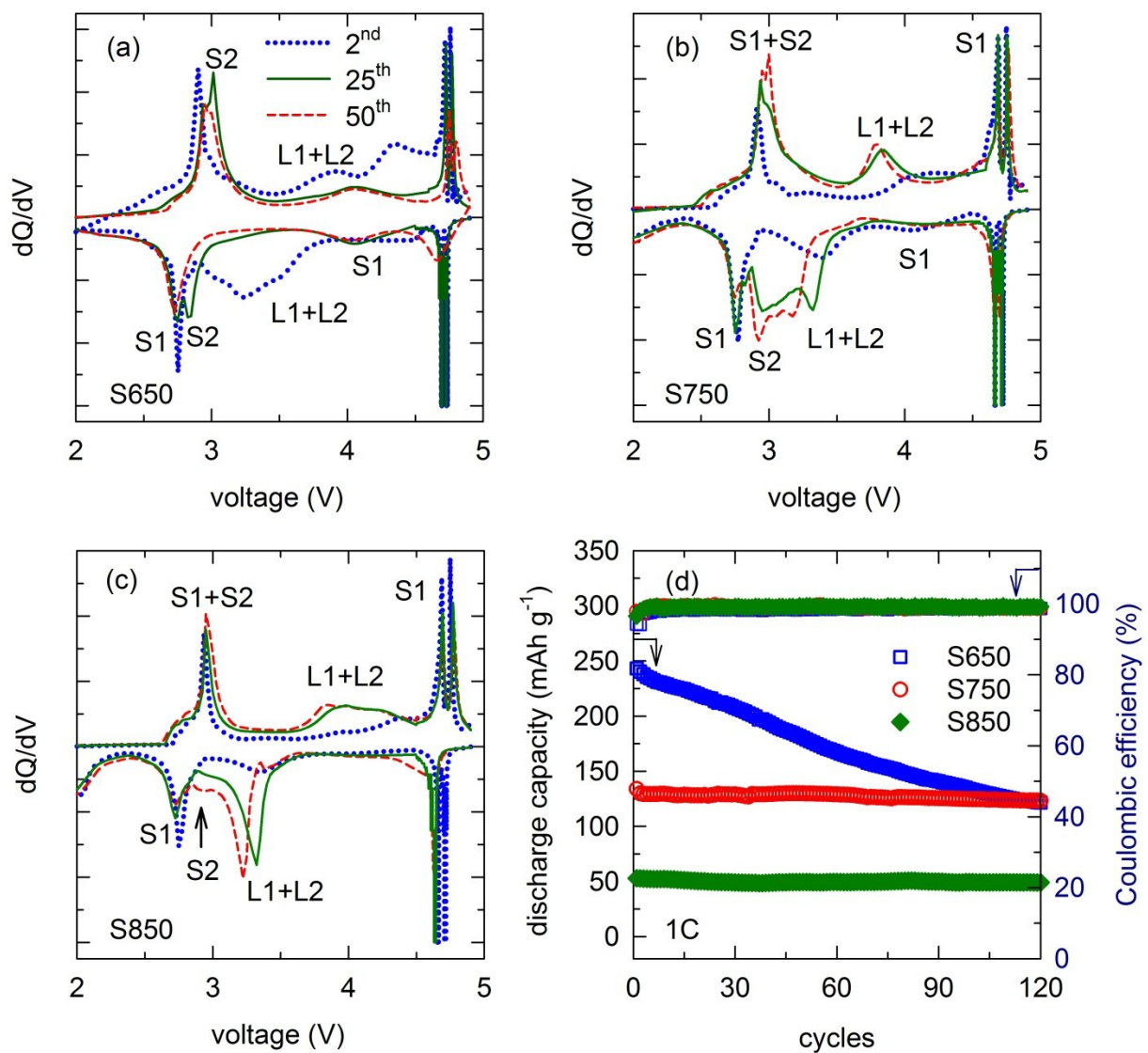


Figure S5. dQ/dV plots of (a) S650, (b) S750, and (c) S850, at C/20 over a 2.0–4.9 V voltage window for the 2nd, 25th, and 50th cycles. S1, S2, L1, and L2 stand for $\text{LiMn}_{1.5}\text{Ni}_{0.5}\text{O}_4$, the new spinel phase, Li_2MnO_3 , and $\text{LiNi}_{0.5}\text{Mn}_{0.5}\text{O}_2$, respectively. (d) Cycling stability curves of the S650, S750, and S850 samples at 1C over a 2.0–4.8 V voltage window.

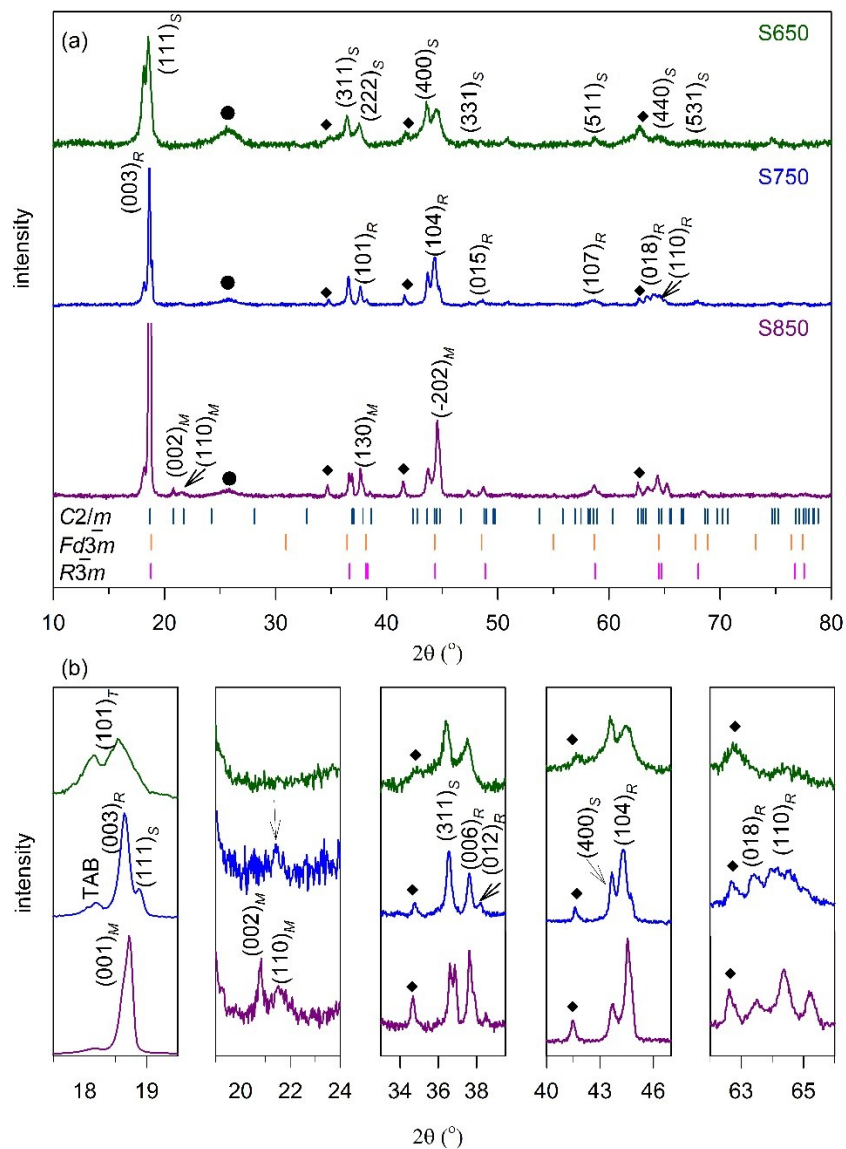


Figure S6. (a) X-ray patterns of S650, S750, and S850 after 50 cycles. The standard marked with $C2/m$ (ICDD entry number 01-084-1634), $Fd\bar{3}m$ (ICDD entry number 01-080-2162), and $R\bar{3}m$ (PDF#09-0063) showed the peak positions correspond to Li_2MnO_3 , $\text{LiMn}_{1.5}\text{Ni}_{0.5}\text{O}_4$ and $\text{LiMn}_{0.5}\text{Ni}_{0.5}\text{O}_2$ components, respectively. (b) Selected 2θ region of XRD patterns for the S650, S750, and S850. The impurity phase of carbon and tetragonal phase were marked with “●” and “◆”, respectively. M , S , R , and T represent for monoclinic, spinel, rhombohedral, and tetragonal, respectively.

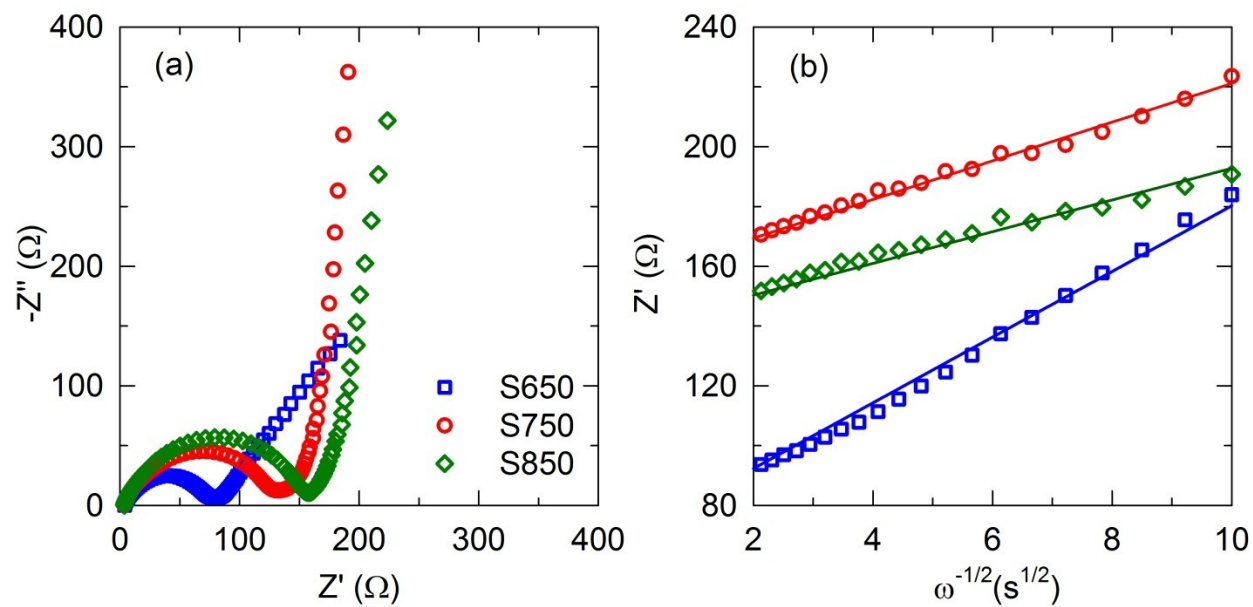


Figure S7. (a) EIS and (b) Real parts of the complex impedance versus $\omega^{-1/2}$ of the S650, S750, and S850 before cycling.

References

1. S.L. Chou, J.Z. Wang, H.K. Liu and S.X. Dou, *J. Phys. Chem. C.*, 2011, **115**, 16220-16227.